nuclear fusion
IAEA

PAPER

Shutdown dose rate benchmarking using modern particle transport codes

To cite this article: T. Eade *et al* 2020 *Nucl. Fusion* **60** 056024

View the article online for updates and enhancements.

IOP ebooks™

Bringing together innovative digital publishing with leading authors from the global scientific community.

Start exploring the collection–download the first chapter of every title for free.

This content was downloaded from IP address 194.81.223.66 on 20/04/2020 at 11:33

IOP Publishing | International Atomic Energy Agency Nuclear Fusion

Nucl. Fusion **60** (2020) 056024 (16pp) https://doi.org/10.1088/1741-4326/ab8181

Shutdown dose rate benchmarking using modern particle transport codes

T. Eade, B. Colling, J. Naish, L.W. Packer and A. Valentine

Culham Centre for Fusion Energy, Culham Science Centre, Abingdon, United Kingdom of Great Britain and Northern Ireland

E-mail: tim.eade@ukaea.uk

Received 10 December 2019, revised 28 February 2020
Accepted for publication 19 March 2020
Published 20 April 2020

Abstract

Shutdown dose rate calculations provide an essential input to the design and research of fusion power plant technology. They allow the estimation of dose to personnel and equipment during planned and unplanned maintenance. The mesh coupled rigorous 2 step (MCR2S) methodology used at Culham Centre for Fusion Energy (CCFE) was originally developed to link the MCNP particle transport code and the FISPACT-II inventory code. As new particle transport codes are developed there is a strong motivation to move towards a code agnostic approach. This paper details the integration of MCR2S with the FISPACT-II API and two other transport codes, Serpent 2 and OpenMC. Two benchmarks, the FNG shutdown dose rate experimental benchmark and the ITER computational benchmark, have been performed and compared to results produced with MCNP. In general, the results show that MCNP, Serpent 2 and OpenMC give shutdown dose rate results similar to the FNG experiment for both experimental campaigns. However, all codes appeared to slightly overestimate the dose rates for Campaign 1 (all results had a C/E between 1 and 1.5) and underestimate the dose rates for Campaign 2 (all results had a C/E between 0.6 and 1). Differences were seen between OpenMC and MCNP for the ITER port plug benchmark, where the lack of variance reduction in OpenMC meant that the neutron flux estimates at the rear of the model were not converged. This led to differences of up to 13% in the shutdown dose rates. It was shown that Serpent 2 and MCNP, where variance reduction was used, gave shutdown dose rates within 3% of each other. Although some areas for development of the Serpent 2 and OpenMC transport codes have been highlighted, overall the comparisons give confidence that the implementation of these two transport codes into the MCR2S work-flow has been carried out successfully.

Keywords: MCR2S, Serpent 2, OpenMC, neutronics, shutdown dose, ITER, FNG

(Some figures may appear in colour only in the online journal)

1. Introduction

As fusion reactors develop into electricity producing power plants, an essential consideration will be the resulting radiation environment they produce and operate in. Not only will 14.1 MeV neutrons be emitted from the deuterium-tritium reaction (currently the most promising for power generating reactors), there will also be significant gamma fields during off-load operations.

Unlike fission plants where the fuel and fission products are the main source of heat and radiation when the reactor is turned off, the radiation fields in fusion plants during shutdown are due to the activated material within the reactor. Components become activated due to neutron capture reactions leading to unstable nuclei. These unstable nuclei usually decay via emission of a particle (gamma, beta or alpha). For the protection of personnel and equipment, external dose from photons are a primary consideration.

Significant effort has been made into predicting the radiation levels in fusion reactors during shutdown. At present two main approaches are used. These are the 'direct-one-step' or D1S method [1–3] and the 'rigorous-two-step' or R2S method [4]. Both methods have their advantages and disadvantages which are briefly discussed below.

 © 2020 Crown copyright Printed in the UK

The D1S method has been implemented into modified version of the Monte-Carlo N-Particle (MCNP5) [5] code with specially prepared nuclear cross-section data [1]. This allows the decay gamma fields to be calculated directly in a single MCNP calculation. The main advantage of this technique is no flux averaging across the geometry occurs and shutdown gamma particles are started at the exact location of a given reaction. However, the use of specially prepared nuclear cross-section data means that prior knowledge of the important reactions for individual problems is required. Another limitation is that no secondary activation effects are not taken into account which limits the regimes in which this technique can be used.

The R2S method, in comparison, calculates the average flux and spectra in a specified region of the geometry (e.g. a cell or mesh voxel) using a particle transport code such as MCNP. Explicit activation calculations are then carried out for each cell/voxel using an inventory code such as FISPACT-II [6]. The gamma intensity from these activation calculations are then used as a source in a final (separate) particle transport calculation to ascertain the gamma field in the geometry. This approach allows secondary activation effects to be taken into account and can therefore be used on a wide range of regimes. Some limitations of this approach include flux averaging and material mixing which can introduce uncertainties in the source term if not handled correctly.

CCFE has developed a mesh coupled rigorous 2 step (MCR2S) [7] process and code. This approach uses a superimposed mesh tally to record the neutron flux and energy spectrum in voxels across the geometry of interest. Unlike a cell-based approach, the size of these voxels is independent of the geometry allowing for neutron flux gradients across components to be taken into account. The MCR2S process was originally built around the use of MCNP (originally MCNP5 and later updated to MCNP6 [8]) as the particle transport code and CCFE's FISPACT 2007 [9] (later updated to FISPACT-II [6]) as the activation code. Therefore, the current MCR2S workflow puts significant reliance on MCNP6 [8] being available. MCNP6 is developed by Los Alamos National Laboratory (LANL) and distributed by the Radiation Safety Information Computational Center (RSICC) under a single user license. Several other Monte-Carlo based radiation transport codes are being investigated for their potential use to support fusion analyses. Two codes which have potential as an alternative/complementary radiation transport code for applications in the fusion community are Serpent 2 [10] and OpenMC [11].

In order to investigate the potential of OpenMC and Serpent 2 for fusion shutdown dose rate calculations they have been incorporated into the MCR2S process. Two fusion relevant comparisons have then been carried out; one experimental and the other computational. These comparisons are the Frascati Neutron Generator (FNG) shutdown dose rate benchmark [12, 13], which demonstrates the abilities of the code against a physical experiment, and the simple ITER computational benchmark [14], where comparisons to other shutdown dose rate codes are provided and demonstrates their usage on a model comparable in size to an ITER port plug.

It should be noted that due to a lack of variance reduction techniques in OpenMC this paper does not make comment on the calculation run times for each code. However, the performance of individual transport codes is an area of investigation in of itself and it has been shown that OpenMC [11] and Serpent 2 [10] have regimes in which they perform strongly. OpenMC is highly parallelised and has been shown [11] to scale nearly linearly to over 100 000 cores in fission calculations. Serpent 2 has been shown [15] to perform well for fission reactor style calculations (in which the geometry dimensions are small compared to the neutron mean-free-path) where the delta-tracking method, also known as Woodcock tracking [16], can be used to reduce the calculation time significantly.

2. MCR2S implementations

2.1. Definitions

In order to understand how other transport codes have been integrated in the MCR2S process it is first necessary to understand the process. To aid with the explanation the following terms are defined:

(a) MCR2S Process
This is the entire process for calculating shutdown dose rates, including the particle transport and activation steps.
(b) MCR2S Code
This is the code which takes the output from the particle transport calculations (along with material and irradiation data), performs activation calculations for each mesh voxel and subsequently creates the shutdown gamma source. Currently the MCR2S code is an OpenMPI parallelised Fortran program which interfaces with FISPACT-II.
(c) Source Routine
This is a routine which is embedded into the particle transport codes to read the shutdown gamma source and sample locations and energies of starting particles. It also isotropically samples the direction of the starting particles.
(d) Posmat file
A file containing data on the fraction of each material under each voxel of the mesh. It is used by the MCR2S code to mix materials for each voxel in order to perform inventory calculations.

A flow diagram depicting an overview of the basic MCR2S process can be seen in figure 1.

2.2. Updates to MCR2S

Since the original version and first paper was published on MCR2S [7] many improvements have been made to the methodology which have not been publicly documented. The main improvements to the code are therefore discussed here. Larger additional improvements have also been made but in order to keep this paper concise these will be detailed in a later paper.

The original code was a collection of UNIX scripts and Fortran routines for MCNP. The MCR2S code over the years has been rewritten into a single Fortran program. The Fortran program is now written in a modern modularised standard and accelerated using OpenMPI.

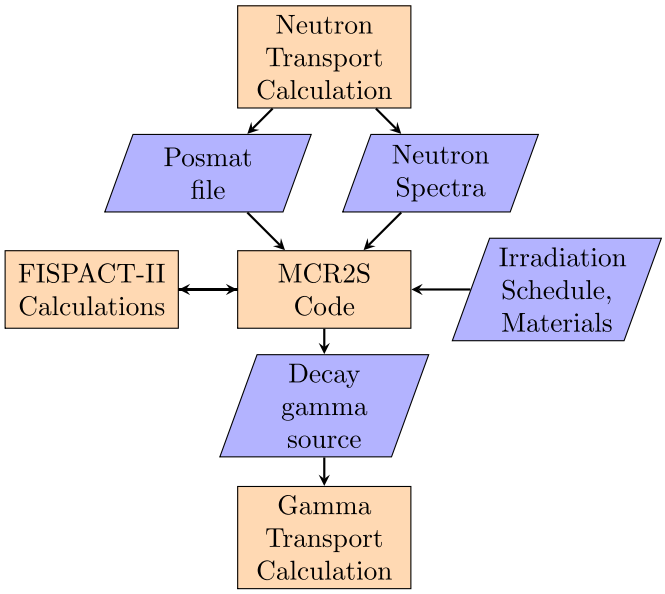

Figure 1. Overview of the basic MCR2S process.

To increase the performance of MCR2S further the code has also been modified to take advantage of the newly developed FISPACT-II Application Programming Interface (API). This API driven approach makes FISPACT-II input and output serialisation redundant, saving considerable time and dramatically reducing disk operations. This can result in significant performance improvements for MCR2S with calculation run times reducing up to eight fold. In order to demonstrate that the results of this new API driven approach are acceptable it has been used for all of the benchmarks reported in this paper.

To track changes made to the code and user reported bugs, the MCR2S code is developed under the 'Git' version control platform. Continuous integration (CI) testing has also been implemented, this performs regression tests every time a modification to the code is made. This gives confidence that changes made to the code do not have unintended consequences.

Capabilities have also been added to allow activation, decay heat and contact dose rate maps to be output directly from MCR2S in a 'VTK' format compatible with common scientific visualisation packages such as VisIT [17]. Another capability allows for the nuclear waste category of each voxel to be calculated and the total waste mass in each category to be output. Waste maps showing the waste category of each voxel can also be created in the 'VTK' output file.

Previously the material under mesh data was obtained using a 'ptrac' approach [7]. This approach used the 'ptrac' card in MCNP to generate a ptrac file containing information on locations of material. The material-under-mesh data is now obtained using a custom subroutine added to MCNP. This custom subroutine randomly samples a user specified number of points in each of the mesh voxels. For each of these points it returns the material present at that point. Once all of the points in a voxel have been picked the fraction of each material in the voxel is calculated and output to the 'posmat' file. The advantage of this newer approach over the old 'ptrac' approach is it is much faster as it has been accelerated via OpenMPI to run on multiple cores, and does not require any particle tracking to take place. The 'posmat' file can be read directly by MCR2S to get the voxel material fractions without any pre-processing, this also saves time compared to the previous 'ptrac' approach which had to be pre-processed by MCR2S before the activation calculations could commence.

It should be noted that other techniques for sampling the material data under a mesh exist. This includes the ray tracing technique, where rays are tracked through each voxel and the track length through each material used to estimate the material fractions. This ray tracing technique has been used and shown to be more computationally efficient. Steps to implement ray tracing material sampling are included in the code development plan, but have not been fully implemented. However, the material sampling processing step is in practice a relatively small fraction of the overall computational effort when compared to the neutron transport and activation calculations.

Furthermore, the original version of MCR2S was limited to the use of rectangular meshes only. MCNP is able to support the use of superimposed cylindrical meshes as well. Support for cylindrical meshes which are useful for some geometry types was added to MCR2S. Although only minor changes were needed to the main MCR2S Fortran code, more significant changes were required for the material sampling routine and the decay gamma source sampling routines in order to sample within cylindrically shaped voxels correctly.

As previously documented [18], MCR2S has also been extended to support MCNP6 unstructured meshes. These meshes define not only the tally region but the geometry itself. Due to the modularised nature of MCR2S the integration of a unstructured mesh routine was relatively straightforward. No changes were required to the material sampling routines as all material information is held in the MCNP6 'eeout' file [19] which also contains results from the neutron calculations. However, new sampling routines were added to the gamma source sampling subroutine.

The MCR2S process has always used a custom subroutine in the particle transport code to sample the gamma intensities file created by the main MCR2S code. Over the years this has been re-written to incorporate support for new features and file formats, such as the European Common Decay Gamma Source (CDGS) format. Some of the new features include support for:

(a) Cylindrical mesh sampling
Support for sampling of cylindrical meshes has been added. These meshes can be off-axis and have an arbitrary origin.
(b) Unstructured mesh sampling
Support for sampling of unstructured mesh has been added. This includes support for all element types supported in MCNP6, including first and second-order tetrahedra, pentahedra and hexahedra.
(c) Source transforms
Support for source transforms has been added. This allows gamma sources to be moved around the geometry to take account of components which have moved during shutdown. Support has also been added for on-the-fly transforms which allows the source to be moved during the

gamma transport calculation, to take account of situations where the activated component is moving e.g. cask transfer etc

(d) Multiple mesh sources
Support for multiple source meshes has been added. This allows multiple meshes to be sampled in a single gamma transport calculation. This can be useful when part of the geometry is moved during shutdown, as transforms can be applied separately to each mesh. It can also be useful when multiple meshes have to be used due to memory constraints in the on-load neutron calculation.

2.3. Modifications for other particle transport codes

In order to accommodate other particle transport codes there are three main interfaces that need to be addressed. These can be seen in figure 1. Two are the input interfaces to the MCR2S code; the 'posmat file' and the neutron spectra. These need to be generated by the transport code. The third is the gamma source file which is generated by the MCR2S code. This needs to be read into and sampled by the transport code. In order to decrease the amount of additional coding and to ensure sampling of the gamma source is the same between codes, a common decay gamma source library was created. This is explained in more detail in section 2.3.1. The input interfaces to the MCR2S code are more radiation transport code specific and are discussed in sections 2.3.2 and 2.3.3, respectively.

2.3.1. CDGS library. A single Commom Decay Gamma Source (CDGS) Library has been written in Fortran with 'C-bindings' to allow for interoperability with other programming languages. The C-bindings allow the subroutines and variables held in the library to be accessed by transport codes written in languages other than Fortran. The CDGS library is transport code independent, i.e. it does not rely on any subroutines or variables from the transport code, and can be used with any programming language which can handle C-bindings, this includes Fortran, C, C++ and Python. The library is based on the original source routine written for MCNP. However, in order to make the library transport code independent, references to any MCNP variables and routines were removed.

The library contains a number of routines including CDGS file reader, mesh selection, voxel selection, position in voxel sampling and energy sampling. Using a user set flag, the mesh and voxel sampling can be performed in one of two ways—either via analogue or uniform sampling techniques. Analogue sampling is analogous to nature, with the mesh and voxel selection based on the intensities of the mesh or voxels. This means more intense/activated meshes/voxels will be picked more frequently by the source sampling routines. With the analogue approach all starting particles are started with a weight of one. Uniform sampling on the other hand picks all meshes and voxels with equal probability. To make the 'game' fair the weight of the starting particle is then adjusted to take account of the relative intensity of the mesh/voxel being sampled. Whereas analogue sampling performs well when the shutdown dose rate tally is close to the most active parts of the model, uniform sampling performs better when the shutdown dose rate tally is situated away from the most active parts of the model.

All of the routines contained in the CDGS library have explicit interfaces, therefore a calling routine will pass a number of defined variables into the routine and receive back a defined result such as a mesh or voxel id, or starting particle position.

A transport code dependent wrapping subroutine is needed to drive the library. This transport code dependent subroutine calls the various routines in the library with random numbers, taken from the transport code random number generator, to sample source particles. This code dependent subroutine also uses the transport codes internal routines to check whether a source particle is within a void or importance zero region and perform rejection sampling if it is.

2.3.2. Serpent 2. Serpent 2 [10] is a modern transport code developed by the Technical Research Centre of Finland (VTT) originally for reactor physics burn-up calculations. Additions have been made to Serpent 2 to allow fixed/external sources to be used for shielding and other particle transport applications. This opened the possibility to use Serpent 2 for fusion research and an activity as part of the EUROfusion Power Plant Physics and Technology (PPPT) work programme is evaluating its capability and performance. Serpent 2 is currently in development and no production release is available. Version 2.1.31 beta was therefore used for all calculations presented in this paper.

Like MCNP, Serpent 2 has a superimposed rectangular and cylindrical mesh tally capability, although it is limited to only uniform voxel sizes. Without modification to Serpent 2 these superimposed mesh tallies are able to record the neutron flux and energy spectrum across the geometry and output the results to a 'detector' file. Although it contains the same information as the 'meshtal' MCNP file, the Serpent 2 file has a differing format. It was therefore necessary to write a new subroutine for the MCR2S code which was capable of reading the results stored in the Serpent 2 detector file and setting the relevant variables in the MCR2S code. This new MCR2S subroutine was added as a new module written in Fortran.

Serpent 2 is written in the C programming language and it was not possible to directly port the 'posmat' routine used in MCNP to acquire the material information for each voxel. It was therefore necessary to develop a new C routine to produce a 'posmat' file. This routine followed the same principles of the Fortran routine written for MCNP. The Serpent 2 routine samples a user selected (default 1000) number of points randomly in each of the voxels. It then uses the Serpent 2 'WhereAmI' function to find the material under each voxel. Once all the points have been sampled the routine statistically estimates the fraction of each material in each voxel. This information is then written to the 'posmat' file in the same format as that written by the MCNP routine. As well as writing the 'posmat' file the new Serpent 2 routine also outputs the material isotopic definitions from the neutron transport calculation numbered consistently with those given in the 'posmat' file.

The third modification to Serpent 2 was the addition of a CDGS library. This involved writing the transport code specific routine in C. Like the 'posmat' routine this was based on the code written for MCNP but replaced the MCNP random number generator for the Serpent 2 random number generator and used the Serpent 2 'WhereAmI' function to check the material and cell of the starting particle.

2.3.3. OpenMC. OpenMC [11] is an open source particle transport code written in C++ and originally developed at MIT. Again, OpenMC, was originally written as a reactor physics code and is currently being actively developed by the community (including CCFE) for other particle transport applications. A production version of the code has not yet been released. Here, version 0.12.0-dev [20] was used for the calculations presented in this report.

One of the advantages of OpenMC is it is written in C++ in a modern object orientated manner which allows for Application Programming Interfaces (API) to be created. A Python API is currently available and can be used to script calculations and results processing. This can be particularly useful when performing parameter studies.

OpenMC, like MCNP and Serpent 2, also has a superimposed rectangular mesh tally capability. Without modification to OpenMC the superimposed mesh tally results are stored in the HDF5 binary file. These can be read in and manipulated using the OpenMC Python API. In order to interface the neutron flux results with MCR2S code it was decided that the mesh tally results would be converted from the HDF5 format into a MCNP 'meshtal' format. This was done using a Python script and the OpenMC API. This converted mesh tally could then be directly read in to MCR2S without any modification to the MCR2S Fortran code. In the work presented here this was done for proof of concept and ease of implementation however, in the future it may be beneficial to read the mesh data directly from the OpenMC HDF5 file straight into MCR2S which would remove an unnecessary step from the process.

Like MCNP and Serpent 2 it was necessary to obtain a 'posmat' file from the OpenMC code detailing the location of materials in each mesh voxel. As OpenMC already has the capability to obtain the material information for a structured three-dimensional grid of points, it was decided that a post-processing method would be used to create the 'posmat' file. This meant that OpenMC did not require modification. In order to create a 'posmat' file an OpenMC 3D plotting calculation is carried out. The plotting grid is centred on the neutron mesh tally, with the same extents and a resolution 10 times that of the neutron mesh tally. This means that each voxel has 1000 sampling locations evenly distributed throughout. A Python script was written to process these points and calculate the fraction of material in each voxel. One downside to this approach is that the evenly distributed sampling points can miss material in a voxel, especially when there is a small slice of material on one side of the voxel. This approach also means voxels are required to be the same size across the entire mesh and the Python script is slow to sort through all of the voxels. This approach was taken due to the ease of implementation but in the future it would be beneficial to update to the approach to use a method based on random sampling and take a parallelised approach.

The final requirement is for the integration of the CDGS library into OpenMC. This is to enable the sampling of shutdown gamma source particles from the CDGS file. To be able to do this a certain version [20] of OpenMC was required. This version of OpenMC has a new source capability that allows source particles to be sampled from a user defined shared library file. Therefore, a code dependent subroutine was written in C++ to wrap the CDGS library in a similar way to the one written for Serpent 2; but using the OpenMC random number generator and 'where am I' functions. The OpenMC specific C++ subroutine and CDGS library were then compiled into a shared library file that could be pointed to during the OpenMC gamma calculations.

3. Shutdown dose rate comparisons

3.1. FNG ITER shutdown dose rate benchmark

3.1.1. Description. The Frascati Neutron Generator (FNG) facility uses deuteron beams accelerated up to 300 keV which are focused onto a tritiated titanium target to produce 14.1 MeV neutrons. Two experimental campaigns took place during the year 2000 to irradiate a material assembly designed to create a neutron flux spectrum similar to that anticipated in the outer vacuum vessel region of ITER.

The layout of the assembly can be seen in figure 2 and consisted of a block of stainless steel and water-equivalent (Perspex) material with a total thickness of 714 mm and a lateral size of 1000 mm x 1000 mm. The exact material definitions used in the particle transport and activation calculations can be found in the Shielding Integral Benchmark Archive and Database (SINBAD) [13]. A cavity was arranged within the block (126 mm $\times$ 119 mm) behind 224.7 mm of the shield. A void channel of 27 mm inner diameter was created between the source and the void chamber.

Models for OpenMC and Serpent 2 were converted from the MCNP model provided in SINBAD [13]. Stochastic volume calculations were performed with Serpent 2 and OpenMC. The results of which were compared to a stochastic volume calculation performed with MCNP. The majority of the Serpent 2 and OpenMC cell volumes were within 2% of the MCNP values and all within 10%. It was also found that 95.65% and 94.98% of the OpenMC and Serpent 2 cell volumes respectively were within two standard deviations of the MCNP result; as would be expected from a Gaussian distribution. Along with zero lost particles in 1×10^{-9} this gives confidence in the fidelity and consistency of the models.

The first experimental campaign recorded several results, including shutdown dose rates using a Geiger–Muller detector and a thermoluminescent dosimeter, and ^{58}Ni reaction rates. The second campaign recorded the dose rate using a special plastic scintillator (NE105) along with the neutron and photon spectra using an NE 213 scintillator. The irradiation histories for the two campaigns are given in table 1.

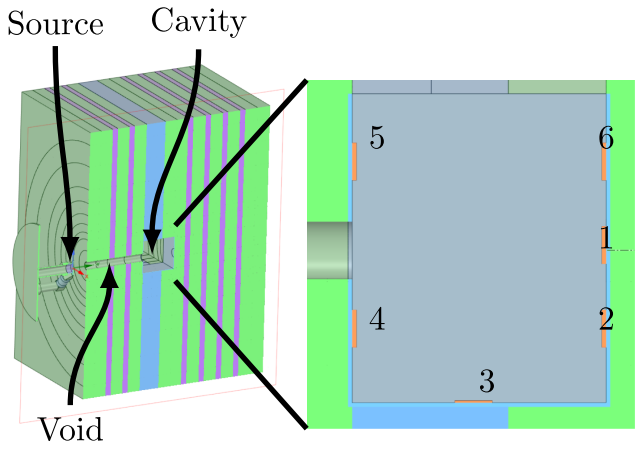

Figure 2. Layout of the FNG shutdown dose rate benchmark.

Table 1. FNG irradiation scenarios for Campaigns 1 and 2.

Campaign 1		Campaign 2	
Strength (n/s)	Duration (s)	Strength (n/s)	Duration (s)
$2.32E+10$	19440	$3.04E+10$	17480
$0.00E+00$	61680	$4.28E+10$	7820
$2.87E+10$	32940	$0.00E+00$	54140
$0.00E+00$	54840	$4.29E+10$	22140
$1.90E+10$	15720	$0.00E+00$	900
$0.00E+00$	6360	$3.78E+10$	3820
$1.36E+10$	8940	$0.00E+00$	420
		$2.86E+10$	140

Full descriptions of the two campaigns including the materials specifications, source specification, experimental results can be found in SINBAD [13].

The FENDL3.1d [21] nuclear data cross-section library was used in all the transport codes. It should however be noted that although MCNP and Serpent 2 both used the ACE (A Compact ENDF) files, OpenMC requires this data to be converted to a HDF5 file before it can be used. The EAF-2010 [22] activation library was used in all FISPACT-II calculations. Although the conversion of the ACE files to a format suitable for OpenMC was not checked, the use of the same nuclear data in all codes minimises the differences seen in the results due to the nuclear data.

3.1.2. Results campaign 1. The results for Campaign 1 are presented in this sub-section. The reaction rates for the six nickel foils in the central cavity are presented in table 2 and 3 for ^{58}Ni(n,p)^{58}Co and ^{58}Ni(n,2n)^{57}Ni reactions respectively. Calculation over experimental results can be seen in figures 3 and 4 for the ^{58}Ni(n,p)^{58}Co and ^{58}Ni(n,2n)^{57}Ni reactions respectively. It should be noted that the error bars on the C/E values are the statistical error on the Monte-Carlo transport calculations. The pink error band in the figures is the 4.5% error quoted on the experimental results.

The ^{58}Ni(n,p)^{58}Co reaction rates compare well to the experimental results. The reaction rates of all foils fit within one standard deviation of the experimental and calculation uncertainty for both the MCNP and Serpent calculations. It should be noted that although run for the same number of starting particles the Serpent 2 results have higher statistical errors than MCNP and OpenMC. This may be due to the type of tally used in the Serpent 2 calculation. For MCNP and OpenMC track length estimator tallies were used to estimate the reaction rates in the foils. However, due to the way Serpent 2 performs the geometry tracking, using the delta-tracking technique [16], it is necessary to use collision flux estimators which score only when an interaction occurs. As the foils are thin, and interaction are therefore less likely to occur, track length estimators are more efficient than the collision flux estimators used in Serpent 2.

The OpenMC results overestimate the reaction rate for Foils 1, 5 and 6. OpenMC also slightly overestimates the reaction rate for Foil 3. The statistical errors on the OpenMC results are less than a 1% which is an indication that the solution is converged. However, unlike MCNP which has 10 statistical checks, including checks on the mean behaviour, relative error, variance of the variance, figure of merit and probability density slope, OpenMC does not have any additional convergence tests. Therefore unlike the MCNP results, which passed all 10 statistical checks, it is not possible to say with confidence that the OpenMC results are converged. As a result, it is not clear what is the exact cause of these slight differences, as it may just be down to a convergence issue. It should be noted that all OpenMC results are all still within 15% of the experimental mean giving some confidence that the code is transporting neutrons correctly.

The ^{58}Ni(n,2n)^{57}Ni reaction rates have worse agreement with the experimental results. Only 50% of the MCNP results fit within one standard deviation of the experimental results. The reaction rates for the other foils are too low. Only the Serpent 2 ^{58}Ni(n,2n)^{57}Ni reaction rate for Foil 3 fits within one standard deviation of experimental result. Serpent 2 generally underestimate the reactions rates by up to 9% when compared to MCNP. Like MCNP, only 50% of the OpenMC results fit within one standard deviation of the errors. The reaction rates for the remaining three foils (1, 2, 4) are underestimated by OpenMC. The predicted reaction rates for Foils 5 and 6 from OpenMC are higher than those of MCNP and Serpent 2; suggesting a difference in the neutron flux and spectrum predicted by the codes in these areas.

The shutdown photon dose rate in the cavity for Campaign 1 was measured using a Geiger–Muller detector. The Geiger–Muller detector was approximated in the MCNP, Serpent 2 and OpenMC calculations with two spheres, an outer aluminium spherical shell of 0.1 cm and a void sphere of 1.9 cm. The dose rate was calculated using a flux tally with the ITER recommended ICRP74 [23] dose conversion factors applied. This was the same for each transport code.

The experimental and calculated dose rates for Campaign 1 are given in table 4 and presented as C/E values in figure 5. In figure 5 the pink band is the experimental error and the error bars on the C/E points are the statistical error on the photon transport runs which are generally less than 1% for all codes and decay times. It should be noted that there are

Table 2. FNG ^{58}Ni(n,p)^{58}Co foil experimentally measured and calculated reaction rates (x10^{-24}/source neutron).

	Experiment	MCNP		Serpent 2		OpenMC	
Foil	RR	RR	Err	RR	Err	RR	Err
1	2.15×10^{-05}	2.16×10^{-05}	5.62×10^{-08}	2.25×10^{-05}	6.24×10^{-07}	2.34×10^{-05}	4.42×10^{-08}
2	5.19×10^{-06}	5.49×10^{-06}	3.08×10^{-08}	5.30×10^{-06}	2.53×10^{-07}	5.21×10^{-06}	3.39×10^{-08}
3	4.13×10^{-06}	4.10×10^{-06}	4.60×10^{-08}	3.77×10^{-06}	2.87×10^{-07}	4.35×10^{-06}	4.77×10^{-08}
4	8.48×10^{-06}	8.61×10^{-06}	4.13×10^{-08}	8.47×10^{-06}	2.85×10^{-07}	8.03×10^{-06}	4.09×10^{-08}
5	7.86×10^{-06}	7.83×10^{-06}	3.91×10^{-08}	7.81×10^{-06}	3.82×10^{-07}	8.99×10^{-06}	4.41×10^{-08}
6	5.15×10^{-06}	4.90×10^{-06}	2.94×10^{-08}	4.98×10^{-06}	2.65×10^{-07}	5.68×10^{-06}	3.50×10^{-08}

Table 3. ^{58}Ni(n,2n)^{57}Ni foil experimentally measured and calculated reaction rates (x10^{-24}/source neutron).

	Experiment	MCNP		Serpent 2		OpenMC	
Foil	RR	RR	Err	RR	Err	RR	Err
1	2.84×10^{-06}	2.36×10^{-06}	6.14×10^{-09}	2.35×10^{-06}	6.17×10^{-08}	2.47×10^{-06}	3.01×10^{-09}
2	3.94×10^{-07}	3.86×10^{-07}	2.40×10^{-09}	3.43×10^{-07}	2.11×10^{-08}	3.28×10^{-07}	2.32×10^{-09}
3	2.07×10^{-07}	1.98×10^{-07}	3.44×10^{-09}	1.90×10^{-07}	2.47×10^{-08}	2.10×10^{-07}	3.46×10^{-09}
4	4.92×10^{-07}	4.96×10^{-07}	2.73×10^{-09}	4.38×10^{-07}	2.13×10^{-08}	4.24×10^{-07}	2.65×10^{-09}
5	4.71×10^{-07}	4.25×10^{-07}	2.51×10^{-09}	3.89×10^{-07}	2.48×10^{-08}	4.97×10^{-07}	2.53×10^{-09}
6	3.64×10^{-07}	3.18×10^{-07}	2.16×10^{-09}	3.13×10^{-07}	2.17×10^{-08}	3.81×10^{-07}	2.66×10^{-09}

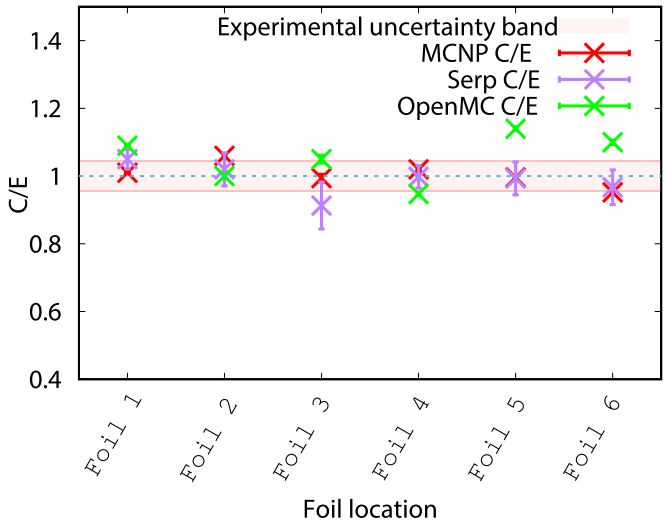

Figure 3. C/E Plots of the ^{58}Ni(n,p)^{58}Co foil reaction rates.

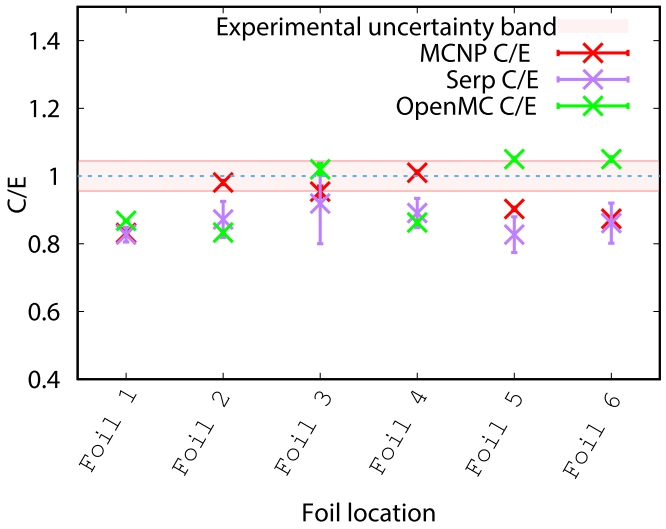

Figure 4. C/E Plots of the ^{58}Ni(n,2n)^{57}Ni Foil Reaction rates.

other contributing errors on the calculated results such as the nuclear data uncertainties, modelling inaccuracies and statistical errors on the neutron transport calculations. Currently the combination and propagation of these errors through the R2S method has not been implemented but is an area of active development.

The dose rates predicted by all of the transport codes are higher than that measured with the Geiger–Muller detector. OpenMC predicts dose rates in line with MCNP for all but the 1 day decay time. This is despite the difference in the way the 'posmat' file has been created with OpenMC. In OpenMC the small amount of material in the voxels on one edge of the central chamber has not been sampled and therefore these voxels have not been activated. This difference can be seen in the plots of the activity for OpenMC and MCNP in figure 6, at the y = 40 cm position. However, as the piece of material is only 0.5 mm thick it does not contribute significantly to the dose rate in the centre of the cavity. A different sampling methodology for the 'posmat', similar to that used in MCNP or Serpent 2, would remove this discrepancy and should form part of further work as the OpenMC R2S work-flow progresses.

The Serpent 2 results are lower than those predicted by MCNP. This is mainly down to the generated gamma source term. Analysing a single voxel at the rear of the cavity, in line with the streaming path, the total gamma intensities are

Table 4. Shutdown dose rate in the cavity of the FNG mock-up (results in μSv/h and errors are the statistical error on the gamma transport calculation).

Decay Time	Experiment	MCNP		Serpent 2		OpenMC	
Days	Dose	Dose	Err	Dose	Err	Dose	Err
1	$2.46 \times 10^{+00}$	$3.40 \times 10^{+00}$	1.16×10^{-02}	$3.17 \times 10^{+00}$	2.93×10^{-02}	$2.95 \times 10^{+00}$	5.97×10^{-03}
7	6.99×10^{-01}	9.10×10^{-01}	3.55×10^{-03}	8.30×10^{-01}	9.12×10^{-03}	8.92×10^{-01}	3.05×10^{-03}
15	4.95×10^{-01}	7.17×10^{-01}	2.80×10^{-03}	6.70×10^{-01}	7.20×10^{-03}	7.18×10^{-01}	2.55×10^{-03}
30	4.16×10^{-01}	6.14×10^{-01}	2.33×10^{-03}	5.58×10^{-01}	6.58×10^{-03}	6.18×10^{-01}	2.37×10^{-03}
60	3.16×10^{-01}	4.71×10^{-01}	1.79×10^{-03}	4.45×10^{-01}	5.06×10^{-03}	4.68×10^{-01}	1.04×10^{-03}

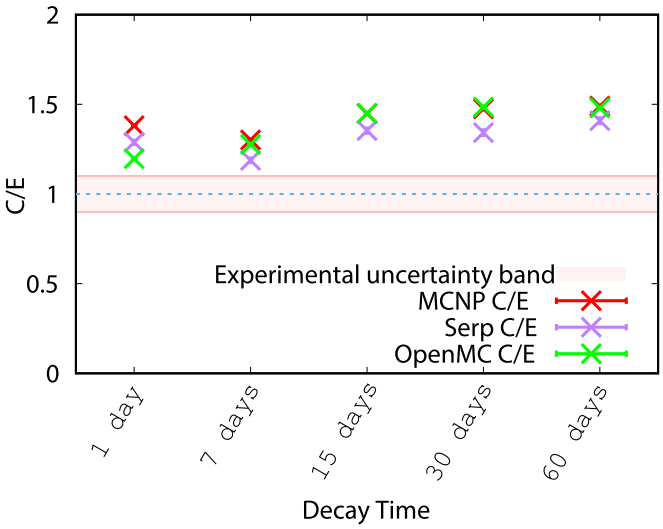

Figure 5. C/E Plots of the shutdown dose rate for Campaign 1 at various decay times.

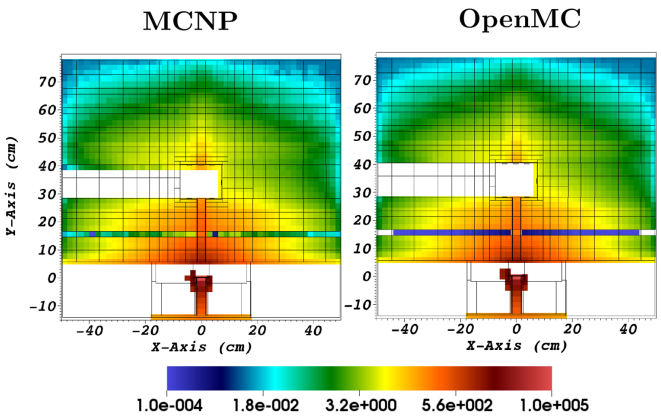

Figure 6. Total activity (Bq/g) through the x-y plane of the FNG model, Right: OpenMC result. Left: MCNP result. Shows missing activation along the rear of the central chamber around y = 40 cm in the OpenMC model caused by the non-random sampling used for the creation of the OpenMC 'posmat' file.

very similar between Serpent 2 and MCNP, however there is up to a 5% difference in values for the individual energy bins. As the same nuclear data (EAF2010) and activation code (FISPACT-II) have been used for both MCNP and Serpent 2 activation calculations, this difference must be down to differences in the neutron flux spectrum predicted by the two codes. It should also be noted that there is a difference in the photon physics models used by the two codes [24] which may have a small effect on the Serpent 2 results. Differences have been observed in bremsstrahlung production; where MCNP treats both positron and electrons identically, Serpent 2 treats positrons and electrons as two separate particles types. As positrons have a lower yield compared to electrons this may partially explain why we see lower dose rates in the central cavity for Serpent 2.

Previous analysis of the FNG ITER shutdown dose rate benchmark using MCR2S [7] showed C/E values closer to 1. However, this paper is not aimed at improving upon the benchmarking previous performed as there are some details of the calculations performed which were not optimally configured. This includes the fitting of the mesh tally and the dose conversion factors used. During the previous analysis the neutron mesh tally was fitted perfectly to the geometry i.e. there were no voxels that overlapped material and void. This prevented any flux mixing and therefore improved the results. As mentioned previously the workflows with OpenMC and Serpent 2 are limited to uniform voxel sizes; this means fitting the mesh exactly to the geometry was not possible with all three of the codes. Therefore, to ensure fairness between the codes the same uniform mesh was used in all three cases. This uniform mesh had some voxels which overlapped material and void within the cavity. As the neutron flux is higher in the void it will artificially increase the activation of the material in the cavity wall and therefore increase the shutdown dose rate. There is also a difference in the gamma to dose conversion factors used between this and previous analysis. Previously [7] the ANS-1977 and 1991 factors were used, in this analysis the ITER recommended ICRP74 values have been used. These factors can make a significant difference to the results. However, confidence can be gained from the fact that in this analysis Serpent 2 and OpenMC give similar results to MCNP. Therefore, if the calculations were optimised in a similar fashion to the previous MCNP calculations [7] there is reason to expect the OpenMC and Serpent 2 calculations will predict C/E values closer to 1.

3.1.3. Results campaign 2. For the second campaign the dose rate was recorded in the central chamber using a plastic scintillator detector. This plastic scintillator was introduced into the central chamber of the model as a cylindrical volume

Table 5. Shutdown dose rate in the cavity of the FNG mock-up (results in μSv/h).

Decay Time	Experiment	MCNP		Serpent 2		OpenMC	
Secs	Dose	Dose	Err	Dose	Err	Dose	Err
4380	4.88E+02	3.48E+02	6.26E–01	3.28E+02	1.22E+00	3.50E+02	6.62E–01
6180	4.15E+02	3.05E+02	5.49E–01	2.85E+02	1.08E+00	3.06E+02	3.52E–01
7488	3.75E+02	2.76E+02	4.97E–01	2.39E+02	3.02E+01	2.80E+02	2.86E–01
11 580	2.68E+02	2.05E+02	3.69E–01	1.85E+02	2.69E+01	2.06E+02	2.61E–01
17 280	1.73E+02	1.36E+02	2.44E–01	1.22E+02	5.10E–01	1.36E+02	2.57E–01
24 480	1.01E+02	8.05E+01	1.53E–01	7.14E+01	3.07E–01	8.07E+01	9.77E–02
34 080	5.06E+01	4.12E+01	8.24E–02	3.60E+01	1.66E–01	4.09E+01	8.37E–02
45 780	2.30E+01	1.91E+01	4.20E–02	1.64E+01	8.05E–02	1.90E+01	1.79E–02
57 240	1.17E+01	9.78E+00	2.45E–02	8.22E+00	4.58E–02	9.59E+00	2.03E–02
72 550	5.80E+00	5.01E+00	1.40E–02	4.11E+00	2.51E–02	4.85E+00	1.32E–02
90 720	3.56E+00	3.14E+00	9.41E–03	2.49E+00	1.62E–02	3.02E+00	6.99E–03
132 000	2.43E+00	2.18E+00	6.55E–03	1.69E+00	1.09E–02	2.12E+00	5.62E–03
212 400	1.78E+00	1.62E+00	4.71E–03	1.26E+00	7.99E–03	1.60E+00	3.23E–03
345 600	1.22E+00	1.15E+00	3.35E–03	8.96E–01	5.56E–03	1.16E+00	3.21E–03
479 300	9.52E–01	9.26E–01	2.78E–03	7.06E–01	4.36E–03	9.40E–01	2.79E–03
708 500	7.59E–01	7.37E–01	2.21E–03	5.63E–01	3.45E–03	7.57E–01	1.13E–03
1050 000	6.67E–01	6.39E–01	1.92E–03	4.87E–01	3.06E–03	6.60E–01	1.53E–03
1670 000	6.13E–01	5.72E–01	1.72E–03	4.32E–01	2.71E–03	5.92E–01	1.12E–03
1710 000	6.14E–01	5.67E–01	1.70E–03	4.30E–01	2.68E–03	5.86E–01	1.75E–03

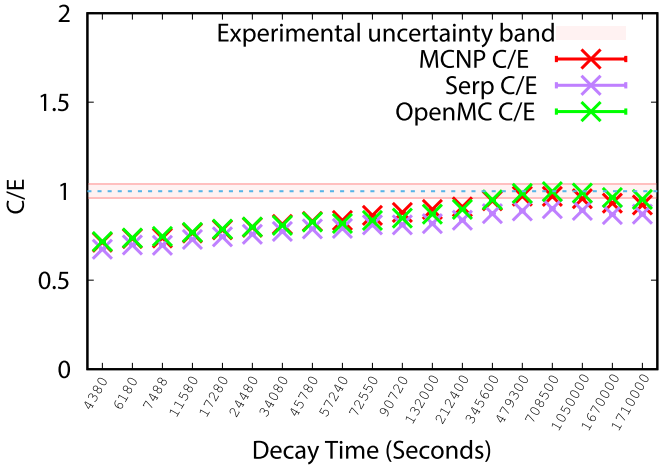

Figure 7. C/E Plots of the shutdown dose rate for Campaign 2 at various decay times.

46 mm high and 46 mm in diameter. It was composed of 52.34 at-% H and 47.66 at-% C with a mass density of 1.037 g/cm^3. The gamma spectrum was measured using a NE 213 liquid scintillator. This was modelled in the central chamber as a 38 mm high and 38 mm diameter cylindrical volume. The composition of this liquid scintillator was taken to be 54.8 at-% H and 45.2 at-% C with a mass density of 0.874 g/cm^3.

Again, the dose rates were measured in the transport codes using flux tallies with the ICRP74 [23] dose conversion factors applied. The factors were the same between all of transport codes.

The experimental and calculated dose rates for Campaign 2 are given in table 5 and presented as C/E figures in figure 7.

At short decay times all of the codes predict very similar shutdown dose rates in the plastic scintillator. However, these dose rates are approximately 30% below the measured experimental value. As the experimental error bound is only 3.9% this leads us to believe that there may be an unknown difference between the computational model and the experiment, or an incorrect cross section in the nuclear data. For longer decay times, after 132 000 s the MCNP and OpenMC results are within the 3.9% error band on the calculation. However, the Serpent 2 results remain below the experimental error band for all but the 708 500 s decay time. This under prediction by Serpent 2 when compared to OpenMC and MCNP is the same as Campaign 1. This strengthens the conclusion that the under prediction is systematic and mainly due to the neutron spectra (the same neutron calculation was used for both Campaign 1 and Campaign 2).

The gamma flux within the liquid NE213 scintillator have also been estimated. The gamma spectrum predicted by the three codes at a decay time of 7 488 s (2.08 hours) is presented in figure 8. The gamma spectrum at 708 500 s (8.2 days) is presented in figure 9. Although presented in SINBAD [25] as a plot, the raw experimental data was not available, therefore the experimental data had to be extracted roughly from the plots and should only be used as a rough guide to the experimental results.

It can be seen at short decay times, figure 8, all three codes produce gamma spectra similar to experimental data. All codes have a peak around the 857 keV, this has previously [25] been attributed to the decay of ^{56}Mn. This is approximately the same as the experimental results. The ^{56}Mn peak around the 1811 keV can also be seen in all of the codes, although it is lower and flatter than the experimental results due to the 24-group energy bin structure used for the gamma source.

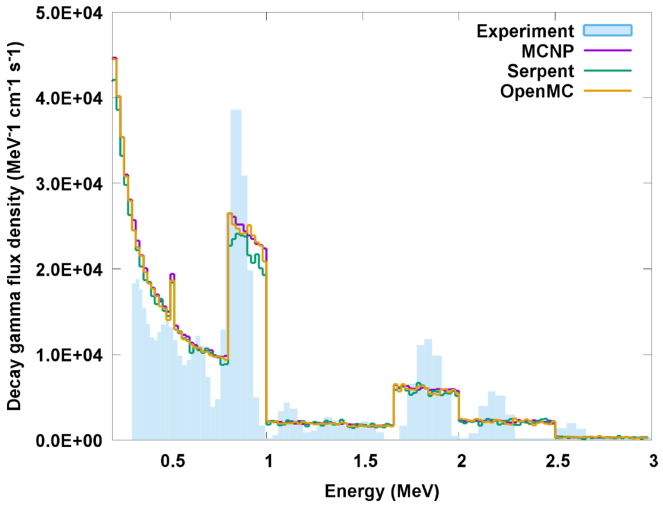

Figure 8. Gamma spectrum from the three codes at a cooling time of 7,488 seconds (2.08 hours).

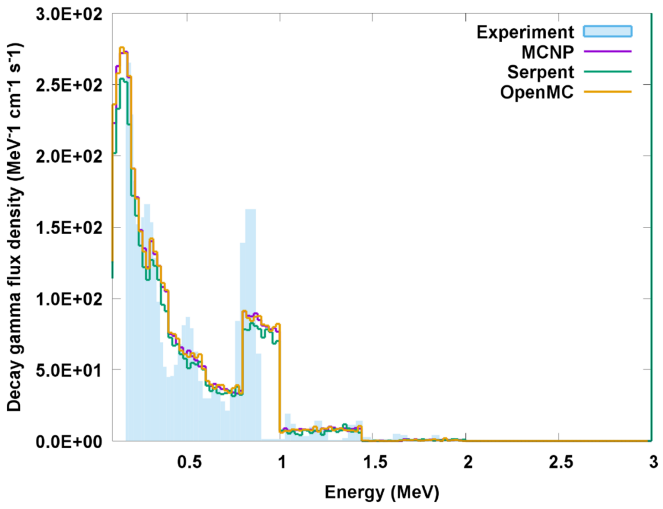

Figure 9. Gamma spectrum from the three codes at a cooling time of 708,500 seconds (8.2 days).

At longer decay times, figure 9, the codes also predict a similar shaped gamma spectrum to the experimental data. However the previously [25] predicted 811 keV ^{58}Co peak is lower and wider in the calculated spectra of all codes. The experimental peaks also appear slightly shifted when compared to the calculated values. This shift was also seen in the original calculations performed in SINBAD [13]. Again, this is due to the gamma source being calculated in a 24-group energy structure which spreads the peak out across the width of the 0.8–1.0 MeV bin. If the peak is at the lower end of an energy bin this makes the spectra look although it is shifted to a higher energy. Although this means that the R2S calculated gamma spectra look different to the experimentally recorded spectra the total gamma energy in the bin should be preserved and therefore the dose rates should not be significantly affected. This is similar for the ^{58}Co peak at 511 keV which is barely visible in the calculated results for OpenMC, MCNP and Serpent 2. The peak around 320.1 keV previously [25] denoted as the ^{51}Cr peak can be seen in the calculations although the actual peaks are lower than those predicted by the experiment.

In the gamma spectra at both 2.08 hours and 8.2 days after shutdown there is a slight discrepancy in the 0.8–1.0 MeV bin for Serpent 2 when it is compared to MCNP and OpenMC. This slightly lower gamma flux is the likely reason for the observed lower shutdown dose rates predicted by Serpent 2 for the second campaign (see table 5).

3.2. ITER computational benchmark

3.2.1. Description. The ITER computational benchmark was created to compare the SDDR predicted by a range of codes and nuclear analysis groups on a simple geometry which represents some of the important aspects of an ITER port plug geometry. This computational benchmark therefore does not provide comparison to actual physical experiments but does allow codes and methods to be compared for an application-relevant geometry.

The computational benchmark [14] is a series of cylinders. The layout of these cylinders is given in figure 10. The outermost cylinder has an inner radius of 50 cm and an outer radius of 100 cm; it is 550 cm in length and is made of steel with a density of 7.93 g cm^{-3}. The first 210 cm (in the axial direction) of the centre of the outer cylinder is filled with a second hollow cylinder made of a steel and water mix with a density of 6.536 g cm^{-3}, this second cylinder has an inner radius of 7.5 cm and an outer radius of 48 cm. The last 15 cm of the centre of the outer cylinder is filled with a third cylinder made of steel. This third cylinder is solid and has an outer radius of 48 cm. There are five concentric circular tallies in the void at the rear of the cylinders. These are 30 cm from the back of the materials and are 10 cm thick. They have outer radii of 15, 30, 45, 60 and 100 cm respectively.

In order to check the consistency of the models for each code, stochastic volume calculations were performed. The volume for each of the cells was calculated and compared to the original MCNP model. These results showed that 86% of the volumes of the cells for the Serpent 2 and OpenMC models were within two standard deviations of the cell volumes of the MCNP model. This is lower than the expected 95% predicted by probability theory but there are only 15 cells in the model. It should also be noted that all Serpent 2 and OpenMC cell volumes are within 1% of the MCNP values and are all are within 3 standard deviations. Along with the zero lost particle rate for each of the models, this gives confidence that the Serpent 2 and OpenMC models are correct to the original MCNP model.

The source is an isotropic 14 MeV neutron source emitted uniformly (in volume) in a 10 cm thick cylinder with an outer radius of 100 cm. This cylinder is positioned 100 cm from the front face of the steel outer most cylinder. See figure 10. The source intensity is 2×10^{-19} n s^{-1}. The cylinders undergo 14 years of irradiation in a schedule similar to the ITER Safety Analysis 2 (SA2) scenario. The exact irradiation is given in table 6.

After irradiation the shutdown dose rate in the four concentric annular tallies is recorded. Along with the shutdown

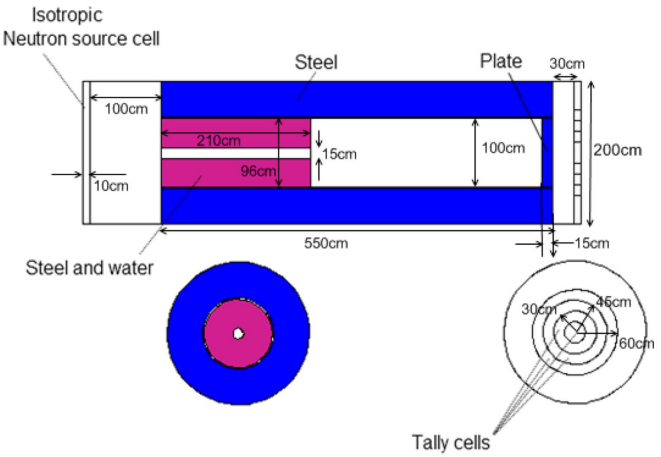

Figure 10. Layout of the ITER computational benchmark.

Table 6. ITER computational benchmark irradiation scenario.

Source Strength (n/s)	Duration	Repetitions
1.07×10^{-17}	2 years	1
8.25×10^{-17}	10 years	1
0	0.667 years	1
1.66×10^{-18}	2 years	1
0	3920 sec	17
2.00×10^{-19}	400 sec	
0	3920 sec	4
2.80×10^{-19}	400 sec	

dose rate, a comparison of the on-load neutron flux spectra at various points along the axis of the cylinder are also compared.

Previous calculations [14, 26, 27] have been performed for the ITER computational benchmark by CCFE, UNED and KIT which show that MCR2S [7], R2Smesh [26] and R2SUNED [27] using MCNP as the transport code give similar answers. This computational benchmark has been repeated using MCR2S with MCNP, Serpent 2 and OpenMC on uniform rectangular meshes. These have then been compared to an MCR2S calculation performed with an MCR2S cylindrical mesh which perfectly fits the cylindrical geometry. It should be noted that currently cylindrical meshes have not been implemented in either the Serpent 2 or OpenMC MCR2S workflows. This is expected to be done in the future.

The regular rectangular meshes used in all transport codes have voxel sizes of $5 \times 5 \times 5$ cm and cover all of the material within the model. It has been shown previously that adjusting the mesh tally to more closely fit the geometry and have finer granularity at the rear allows the results to closer match the cylindrical mesh. However, it is currently not possible to have non-regular rectangular meshes in Serpent 2 or OpenMC (due to the approach taken for generating the 'posmat' file) so to be able to compare results exactly all codes were run with the same mesh. The cylindrical mesh used in MCNP was split into 21 radial bins, 1 angular bin and 112 (5 cm) vertical bins. The boundaries of the mesh were set so they lined up exactly with the cylinders in the geometry. This removes any flux mixing from areas of void and material and should therefore give the most accurate estimation of the shutdown dose rate.

In order to minimise the effect the nuclear data has on the results; FENDL3.1d [21] has been used in all neutron transport calculations and EAF2010 [22] in 175 Vitamin-J energy group structure has been used for all activation calculations. It should again be noted that no checking on the conversion of the ACE files to HDF5 format for OpenMC has been carried out.

3.2.2. Results. The neutron flux and spectra (in Vitamin-J 175 group structure) at 4 locations (x = 112.5, 322.5, 642.5 and 657.5 cm) along the axis (y = 2.5 cm) of the cylinders has been compared for each of the 3 transport codes. The locations and results can be seen in figure 11. For MCNP and Serpent 2 weight windows, generated using a global variance reduction technique [28], were used to increase the efficiency of the calculations and provide better statistics at the rear of the model.

The total neutron flux from the MCNP rectangular mesh shows that the main cause of neutron flux on the closure plate at the back of cylinder is caused by the 15 cm central streaming path. This streaming is an important aspect of the benchmark and it is important to correctly model as it leads to the activation of the rear closure plate which is situated close to the SDDR tallies; and as such provides a large contribution to the SDDR tallies.

The 2 cm gap between the edge of the front cylindrical plug and the outer cylinder also causes significant amounts of streaming along the inner edge of the outer cylinder. This streaming causes activation of the outer cylinder. The activation caused by this streaming is one of the main differences between using a cylindrical mesh and rectangular mesh. As the rectangular meshes do not fit the cylindrical shape exactly, some of the higher flux from the inner void is averaged into the flux in material, this higher average flux is then used to activate the material. The cylindrical mesh exactly fits the geometry so there is no averaging of flux in void and flux in material.

The neutron spectra along the central axis of the benchmark model, shown in figure 11, compares well for OpenMC, Serpent 2 and MCNP at point 1; with Serpent 2 predicting neutron flux results in each energy bin generally within 5% of the MCNP result and OpenMC predicting neutron flux results in each energy bin generally within 15% of the MCNP results (although some bins have differences up to 50%). All predict a very similar level of total neutron flux, with similar 14 MeV and resonance peaks. Serpent 2 and MCNP also predict very similar neutron spectra for points 2, 3 and 4 with the maximum ratio between the estimated flux in a bin being about 2 and generally less than 20%. It should however be noted that OpenMC currently does not have variance reduction capabilities, which is a major limitation in this comparison. This means the neutron flux at points 2, 3 and 4 have a relatively high statistical error in many of the energy bins. In fact OpenMC has 25, 80 and 78 energy bins (below 14.1 MeV) with statistical errors greater than 50% for points 2, 3 and 4 respectively. This is the main reason for the significantly bigger divergence from the MCNP and Serpent 2 results at points 2, 3 and 4. However most OpenMC flux results in each bin are within factor

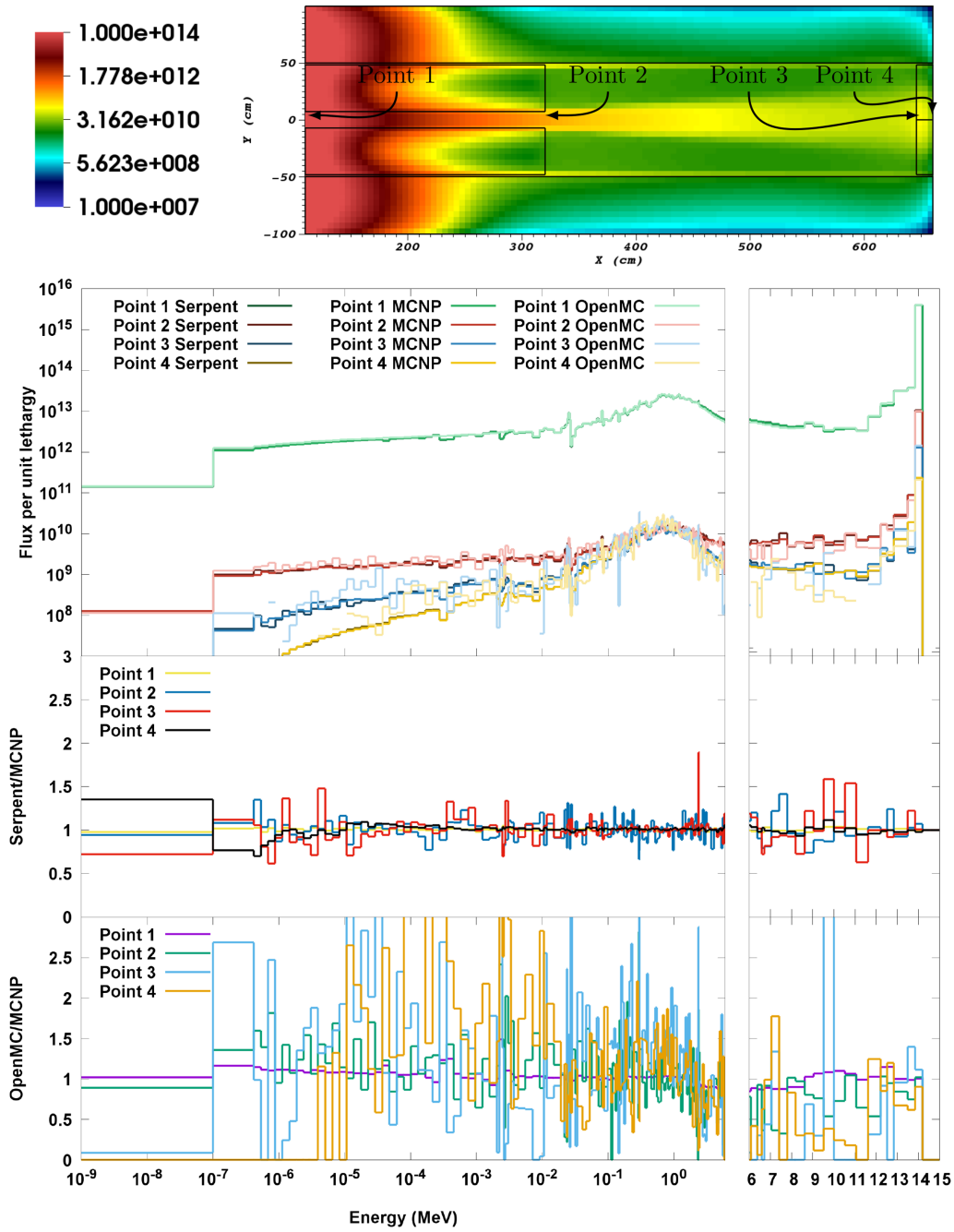

Figure 11. Top: MCNP regular mesh total neutron flux ($n/cm^2/s$). Bottom: neutron spectra at four points through the ITER computational benchmark and ratios of Serpent 2 and OpenMC results to MCNP.

of three of the MCNP results, a fuller assessment can only be made once variance reduction techniques have been added to the code.

The predicted shutdown dose rates in the concentric annular tally cells (i.e. <15 cm radius, between 15 and 30 cm radius, between 30 and 45 cm radius, between 45 and 60 cm radius and >60 cm radius) at the rear of the model can be seen in figure 12. The SDDR results from rectangular meshes (Rec) for all three codes are compared to a cylindrical mesh (Cyl) calculation performed with MCNP. Also presented in figure 12 are results from OpenMC with the Serpent 2 gamma source, these allow us to see what the effect of the lack of the variance reduction on the neutron transport calculation is on the shutdown dose rate results. In order to aid any future studies the shutdown dose rate values are also provided in table 7.

Serpent 2 and MCNP give very similar results for shutdown dose rate in all of the tallies for the rectangular meshes. OpenMC underestimates the dose rate for the inner three tallies. This is due to the difference in neutron flux and spectra predicted by OpenMC when compared to MCNP and Serpent 2; both of which use weight windows to reduce the statistical error on the neutron flux results. When OpenMC is run with the Serpent 2 generated gamma source (for the gamma transport calculation), similar results to Serpent 2 and MCNP

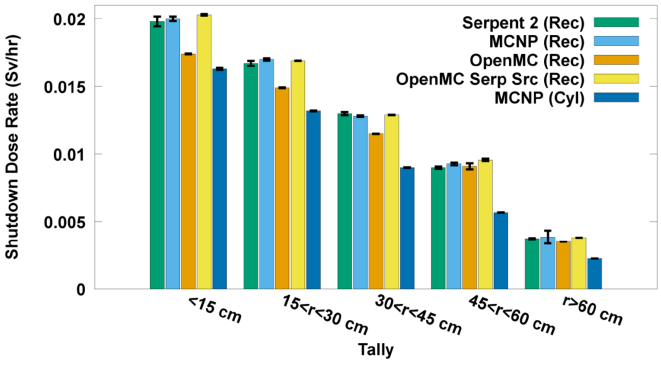

Figure 12. ITER computational benchmark SDDR cell tally results comparison, error bars represent the statistical uncertainty on the gamma transport calculation given by each code.

are obtained. Even with the slight difference in the OpenMC results, the ITER computational benchmark still provides confidence that the MCR2S process has been correctly implemented into Serpent 2 and OpenMC.

It should be noted that the rectangular mesh significantly overestimates the shutdown dose rate in all the tallies when compared to the cylindrical mesh and previous studies [26, 27]. This is because neutron flux averaging occurs in the streaming paths and across the back closure plate. Better agreement could be made by fitting the rectangular mesh more closely to the geometry however, to do this it would be necessary to be able to change the mesh voxel size in certain areas of the model. Currently this is not possible in Serpent 2 or OpenMC (due to the way the 'posmat' file is created). Globally reducing the size of the mesh voxels may help but is not possible for very fine meshes due to memory limitations caused by the necessity to store neutron flux information for 175 energy bins for every voxel. Other methods such as cell-under-mesh [27] developed by UNED are another possible solution, however this requires significant changes to the transport code which have not yet been implemented in OpenMC or Serpent 2.

4. Discussion

The results for the FNG experimental benchmark and the ITER computational benchmark show that OpenMC gives comparable shutdown dose rates to MCNP, Serpent 2 and the experiment. This gives confidence that the MCR2S process has been implemented correctly and can produce reliable results. However, during the calculations a number of issues were highlighted. OpenMC currently does not have efficient variance reduction techniques available. This makes it difficult to perform deep shielding and streaming benchmarks (such as the ITER computational benchmark) as it is difficult to converge the neutron flux and spectra results. Another issue for fusion research calculations (which is currently under development) is the lack of support of toroidal surfaces, this currently limits the calculations which can be carried out—unless a CAD based geometry approach is taken.

Users are also advised that OpenMC batch process and statistical errors quantification are different to those present in Serpent 2 and MCNP. For fixed source calculations OpenMC samples a given number of source particles for the source distribution and then runs these same starting source particles for each batch, using different random numbers for the tracking. The standard deviation for the tallies is then estimated on the difference in result between these batches. This way of calculating the standard deviation means that there is no quantification of the error caused by the source sampling. As a result, users who under sample their source can easily converge on an incorrect answer. This is of particular importance during shutdown dose rate calculations where a large, spatially varying, source must be sufficiently well sampled. This means that for shutdown dose rate calculations there is a trade off between having sufficient numbers of starting particles per batch to sufficiently converge the source and therefore problem, and a sufficient number of batches to allow for the Central Limit Theorem to be applicable in the calculation of the statistical error. In order for the user to be confident that the results obtained are converged additional statistical checks should be added to OpenMC. Currently, only the statistical error is provided as a check for the statistical validity of the results; however from the statistical error alone it is not possible for the user to be confident that their results have converged satisfactorily.

Another inconsistency with OpenMC is that it currently normalises the tallies based on the total weight of the source particles started and not just the number of source particles. This means that a source where all starting particles have a weight of 1 will give the same result as a source where all starting particles have a weight of 0.5. This is presently an issue for uniformly sampled decay gamma sources, which must change the weight of the starting particles. This has been observed to lead to a slight difference in results as the sum of the starting particle weights does not always sum to the number of starting particles.

Serpent 2 was shown to give comparable answers to Experiment and MCNP for the FNG and ITER computational benchmark. Serpent 2 is similar to MCNP in the way that its batch system operates and the tally normalisation is performed; therefore the issues seen in OpenMC regarding the source sampling and source normalisation are not seen. However, users must be aware that in order to get the correct results for fixed source calculations the keyword 'srcrate' must be set to 1. If it is not the normalisation of the tallies during neutron calculations is based on the total loss rate; which means that the tallies cannot just be multiplied by the physical source rate to get results.

It was also found that for Serpent 2 it was difficult to estimate the simulation run times of different models when running in parallel. The optimum number of threads vs OpenMPI tasks are heavily dependent on the model which was being run, the compiler and OpenMPI version.

Like OpenMC, Serpent 2 does not provide any additional statistical checks on the results. This means it is difficult for the user to ascertain whether or not the results have converged. Additional statistical checks should be added to increase the user's confidence that their results have converged.

Table 7. ITER computational benchmark SDDR cell tally results comparison (results in Sv/h).

	MCNP		Serpent 2		OpenMC		OpenMC Serp Src		MCNP Cyl	
Radius	Dose	Err	Dose	Err	Dose	Err	Dose	Err	Dose	Err
< 15 cm	1.98×10^{-02}	3.61×10^{-04}	2.00×10^{-02}	1.68×10^{-04}	1.74×10^{-02}	3.28×10^{-05}	2.03×10^{-02}	5.08×10^{-05}	1.63×10^{-02}	6.52×10^{-05}
15 < r < 30 cm	1.67×10^{-02}	1.86×10^{-04}	1.70×10^{-02}	8.51×10^{-05}	1.49×10^{-02}	2.93×10^{-05}	1.69×10^{-02}	1.64×10^{-05}	1.32×10^{-02}	3.30×10^{-05}
30 < r < 45 cm	1.30×10^{-02}	1.25×10^{-04}	1.28×10^{-02}	5.36×10^{-05}	1.15×10^{-02}	1.30×10^{-05}	1.29×10^{-02}	1.88×10^{-05}	9.01×10^{-03}	2.07×10^{-05}
45 < r < 60 cm	9.00×10^{-03}	8.73×10^{-05}	9.28×10^{-03}	9.75×10^{-05}	9.10×10^{-03}	2.28×10^{-04}	9.58×10^{-03}	1.01×10^{-04}	5.68×10^{-03}	1.31×10^{-05}
r > 60 cm	3.75×10^{-03}	2.82×10^{-05}	3.86×10^{-03}	4.80×10^{-04}	3.52×10^{-03}	5.71×10^{-06}	3.83×10^{-03}	4.36×10^{-06}	2.25×10^{-03}	4.50×10^{-06}

Serpent 2 allows for mesh-based weight window variance reduction techniques to be applied. It can in fact use mesh-based weight windows generated by/for MCNP. A new development in Serpent 2 allows for automatic weight window generation using a built-in response matrix solver [29]. With this new addition it is possible to use an adaptable mesh, (i.e. the size of the mesh voxels is automatically adjusted based on the density, importance or neighbour criteria) which was used for the ITER computational benchmark. The weight window generation is performed using an iterative approach and can produce global variance reduction maps or single/multiple detector reduction.

5. Conclusions

The FISPACT-II API, Serpent 2 and OpenMC have been incorporated into the MCR2S process and benchmarked against the FNG shutdown dose rate experiment and the ITER computational benchmark. The following conclusions have been made from this process:

(a) OpenMC, Serpent 2 and MCNP predict similar reaction rates for the FNG experiment although these are not always in full agreement with the experimental results. OpenMC predicted slightly higher reaction rates for Foils 5 and 6 for both the ^{58}Ni(n,p)^{58}Co and ^{58}Ni(n,2n)^{57}Ni reactions.

(b) The way in which the material information under the mesh is obtained in OpenMC leads to some differences in the generated activation map however this did not have a significant effect on the OpenMC SDDR results. Future work should be performed to allow random (or pseudo random) sampling techniques to be applied as this will minimise the chances of missing material in a mesh voxel.

(c) The calculated shutdown dose rates in the central cavity of the FNG model during Campaign 1 are similar for all codes, although some differences were observed. Serpent 2 underestimates the dose rate in the central cavity when compared to MCNP and OpenMC; which was found to be mainly due to differences in the gamma source which in turn is caused by differences in the calculated neutron spectra. It was also noted that a small contribution to the difference may be due to the different photon physics models used in Serpent 2.

(d) The calculated shutdown dose rates in the central cavity of the FNG model during Campaign 2 are similar for MCNP and OpenMC. For longer time scales the estimated dose rates for OpenMC and MCNP fit within the experimental uncertainty. However, like Campaign 1, Serpent 2 appears to predict lower dose rates than the other two codes; and all except one of the predicted dose rates are outside the experimental uncertainty.

(e) The ITER computational benchmark shows that the codes all predict similar dose rates for an ITER-like geometry. However, as OpenMC does not currently have variance reduction capabilities it is not currently possible to run ITER like calculations in an efficient way. From the neutron spectrum results it can be seen that OpenMC does not converge the neutron flux results particularly well towards the rear of the model.

(f) Apart from a basic estimate of the standard deviation, neither Serpent 2 or OpenMC provide the user with any additional statistical checks to ensure the convergence of the results. Some additional statistical checks should be added to both codes to ensure the user is confident that their results have converged.

(g) It has been shown that OpenMC and Serpent 2 can be used to predict the shutdown dose rates in fusion relevant benchmarks, giving answers that are in reasonable agreement with experiment and MCNP. However, some work is still needed to improve the work-flows, especially for OpenMC, and increase the capabilities including different mesh types/sizes and different material sampling techniques.

Acknowledgments

The authors would like to thank Sam Wareing and Matthew Mavis for their hard work during summer placements at UKAEA; for their help in developing the MCR2S interfaces with Serpent 2 and OpenMC. The authors would also like to thank the development teams of both Serpent 2 and OpenMC for their help in diagnosing and solving problems which occurred during the calculations.

This work has been carried out within the RCUK Energy Programme (grant number EP/T012 250/1). To obtain further information on the data and models underlying this paper please contact PublicationsManager@ccfe.ac.uk. The views and opinions expressed herein do not necessarily reflect those of the UKAEA.

References

[1] Valenza D., Iida H., Plenteda R. and Santoro R. 2001 *Fusion. Eng. Des.* **55** 411–18
[2] Petrizzi L., Iida H., Valenza D. and Batistoni P. 2001 Improvement and benchmarking of the new shutdown dose estimation method by Monte Carlo code (eds) Kling *Advanced Monte Carlo for Radiation Physics, Particle Transport Simulation and Applications* (Berlin: Springer)
[3] Villari R., Batistoni P., Conroy S., Manning A., Moro F. and Petrizzi L. *et al* 2012 *Fusion. Eng. Des.* **87** 1095–100
[4] Chen Y. and Fischer U. 2002 *Fusion. Eng. Des.* **63/64** 107–14
[5] X-5 Monte Carlo Team 2003 *LA-CP-03-0245*
[6] Sublet J.C., Eastwood J. and Morgan J. 2014 *CCFE-R (11) 11*
[7] Davis A. and Pampin R. 2010 *Fusion. Eng. Des.* **85** 87–92
[8] Pelowitz D.B. 2017 *LA-UR-17-29981*
[9] Forrest R.A. 2013 *IAEA INDC(NDS)-645*
[10] Leppanen J., Pusa M., Viitanen T., Valtavirta V. and Kaltiaisenaho T. 2015 *Ann. Nucl. Energy* **82** 142–50
[11] Romano P.K., Horelik N.E., Herman B.R., Nelson A.G., Forget B. and Smith K. 2015 *Ann. Nucl. Energy* **82** 90–7
[12] Batistoni P., Angelone M., Petrizzi L. and Pillon M. 2002 *J. Nucl. Sci. Technol.* **39** 974–7
[13] Kodeli I., Sartori E. and Kirk B. 2006 SINBAD shielding benchmark experiments status and planned activities *ANS*

14th Biennial Topical Meeting of the Radiation Shielding Protection and Shielding Division (Carlsbad, NM, 3–6 April 2006) (https://www.oecd-nea.org/science/wprs/shielding/sinbad/RPSD2006-sinbad.pdf)
[14] Loughlin M. 2011 Loughlin M. 2011 Conclusion of shutdown Dose rate benchmark study Technical Report ITER, 6th ITER Neutronics Meeting (Hefei, China 17–24 June 2011)
[15] Leppanen J. 2017 *Ann. Nucl. Energy.* **105** 161–7
[16] Woodcock E., Murphy T., Hemmings P. and Longworth T. 1965 Techniques used in the GEM code for Monte Carlo neutronics calculations in reactors and other systems of complex geometry *Proc. Conf. Application Computing Methods Reactor Problems* ANL-7050 pp 557 (https://www.yiningkarlli.com/projects/specdecomptracking/references/Woodcock1965.pdf)
[17] LLNL 2019 *Visit User Manual UCRL-SM-220449 Revision 1873e0f 7*
[18] Eade T., Stonell D. and Turner A. 2015 *Fusion. Eng. Des.* **100** 321–33
[19] Martz R.L. 2013 src*The MCNP6 Book On Unstructured Mesh Geometry: User's Guide, LANL Report LA-UR-11-05668 Rev 7*
[20] Davis A. 2019 *commit a419c6e4fb1576df0d1d9f3dcabeb6975cdfc771* (https://github.com/makeclean/openmc.git)
[21] Forrest R.A., Walker C.K., Avirigeanu M., Ignatyuk A. V., Tarkanyi F., Trkov A., Kopecky J. and Fischer U. 2013 *INDC(NDS)-0645*
[22] Sublet J. C., Packer L., Kopecky J., Forest R.A., Koning A. and Rochman D. 2010 CCFE-R 10 05
[23] ICRP 1996 Conversion coefficients for use in radiological protection against external radiation *Ann. ICRP* **26** 3–4
[24] Leppanen J., Kaltiaisenaho T., Valtavirta V. and Metsala M. 2017 Development of a coupled neutron / photon transport mode in the serpent 2 Monte Carlo code *Int. Conf. on Mathematics and Computational Methods Applied to Nuclear Science and Engineering* (Jeju, Republic of Korea, 16–20 April 2017) (https://cris.vtt.fi/en/publications/development-of-a-coupled-neutron-photon-transport-mode-in-the-ser)
[25] Batistoni P., Angelone M., Petrizzi L., Pillon M., Freiesleben H., Richter D., Seidel K., Unholzer S., Chen Y. and Fischer U. 2001 ITER Task T-426
[26] Majerle M., Leichtle D., Fischer U. and Serikov A. 2012 *Fusion. Eng. Des.* **87** 443–7
[27] Sauvan P., Catalan J., Ogando F. and Recio J.S. 2016 *IEEE Trans. Nucl. Sci.* **63** 375–84
[28] Davis A. and Turner A. 2011 *Fusion. Eng. Des.* **86** 2698–700
[29] Leppanen J. 2019 *Nucl. Technol.* **205** 1416–32